Analytical solutions for steady downward flow of a wetting fluid in unsaturated soil using the Adomian decomposition method

Hamed Reza Zarif Sanayei [*,1]

1. Faculty of Engineering, Shahrekord University, Shahrekord, Iran

***Corresponding Author:**
Hamed Reza Zarif Sanayei

Email: hzarif63@gmail.com; zarif@sku.ac.ir
Received: 2025.06.12
Accepted: 2025.07.15
J. Hydraul. Struct., 2025; 12(2): 22-33
DOI: 10.22055/jhs.2025.49954.1355

ABSTRACT

Investigating and simulating the steady water flow in an unsaturated soil column containing oil is one of the most important studies in the field of optimizing oil extraction processes. In order to simulate this flow, governing equation for this field should be solved. The governing equation is strongly nonlinear with limited analytical solutions in the literature. In this paper, analytical solutions have been developed for the nonlinear equation in different soil properties using Adomian Decomposition Method (ADM). A total of three soils with different pore size distribution index are considered in this research. These pore size distribution indexes are 2, 3 and 4 for cases 1, 2 and 3, respectively. Results for the presented analytical solutions are capillary pressure head verses elevation in the unsaturated soil column containing oil. To investigate the accuracy of the derived analytical solutions, capillary pressure head values are obtained from a numerical solution and compared with the presented analytical solution values for all cases. An excellent agreement is observed between analytical and numerical results for three cases. These analytical solutions can be used as a benchmark for verification and efficiency assessment of numerical methods.

KEYWORDS

Analytical solution, ADM, Oil extraction, Unsaturated soil, Capillary pressure head

1. Introduction

Water injection is one of the important methods for increasing oil extraction from underground reservoirs. In this method, the water is injected into an underground reservoir to increase the internal pressure of the reservoir and collect the oil towards the well and the ground surface. Generally, there are two fluid phases in underground oil reservoirs for unsaturated soil zone. These two fluids are oil as the non-wetting fluid and the water as the wetting fluid. Considering this issue, modeling and simulating water movement for underground oil reservoirs is very important for optimal exploitation of oil reservoirs.

In the literature, many researches have been performed to investigate two-phase flow in unsaturated soils. These researches include numerical methods, analytical solutions and experimental studies. Van Duijn et al. [1] analyzed stability of steady, vertically upward and downward flow of water in a homogeneous layer of soil.

In that research, an extension of the Richards equation for investigating dynamic memory effects were considered. Szymkiewicz et al. [2] presented a mathematical model for two phase flow in a heterogeneous porous medium. They investigated this approach with two numerical examples concerning oil–water and CO2–brine flow, respectively. Du and Nydal [3] developed Flow models and numerical schemes for single/two-phase transient flow in one dimension. They presented two numerical schemes in forms of non-iterative and iterative for prediction of transient problems. Cogswell and Szulczewski [4] solved two-phase incompressible flow without capillary potential for large time steps by introducing a macroscopic surface tension and employing a convex energy splitting scheme. They used new homotopy method to increase time step by more than six orders. Zhang et al. [5] presented a numerical simulation of water distribution associated with internal corrosion induced by water wetting in upward inclined oil pipes. In their research, results of numerical simulation were coincided well with available experimental results. Ma et al. [6] developed Fully coupled hydro-mechanical modeling of two-phase flow in deformable fractured porous media based on combining discontinuous Galerkin (DG) and continuous Galerkin (CG) finite element methods (FEM). In their research, several benchmark cases were used for investigating accuracy of proposed method. Ghedira et al. [7] developed numerical simulation of incompressible two-phase flows with phase change process in porous media based on OpenFOAM solver. Their results validated with various test cases. Also, they compared numerical results with analytical solutions and other results in literature.

It should be noted that other numerical techniques have been proposed for investigating two-phase flow in unsaturated soils and/or porous media. These techniques include volume of fluid method (VOF), meshless method, finite volume method (FVM), Lattice Boltzmann method (LBM), Support vector machine (SVM), discontinuous Galerkin method, Green element method (GEM) and/or other numerical methods [8-20]. A number of researchers developed analytical solutions for two-phase flow in unsaturated soils and/or porous media [21-32].

In this study, Adomian Decomposition Method (ADM) is used to develop analytical solutions for steady water flow in an unsaturated soil column containing oil. Governing equation for this flow is strongly nonlinear and therefore, presenting analytical solutions for this equation is very valuable. A total of three soils with different pore size distribution index are considered in this research and analytical solutions by ADM are presented for these cases. These pore size distribution indexes are 2, 3 and 4 for cases 1, 2 and 3, respectively. Also, a comparison of presented analytical solutions with a numerical solution is performed for all cases.

2. Governing equation

The governing equation for steady flow of two fluid phases in unsaturated soil is expressed as [33]:

$$\frac{\partial p_c}{\partial x_i} = \left(\frac{q_{wi}\mu_w}{k_w} - \frac{q_{nwi}\mu_{nw}}{k_{nw}}\right) - (\Delta\rho)g_i \qquad (1)$$

Where p_c, is the capillary pressure and is defined the difference between non-wetting pressure and wetting pressure or $p_{nw} - p_w$, q, is the volume flux, μ, is the dynamic viscosity of fluid, k, is the permeability. In Eq. 1 index w is for wetting phase and index nw is for non-wetting phase. Also, $\Delta\rho$ is the difference between densities for wetting and non-wetting phases, g_i is the gravity acceleration for 3d and x_i, is the directions in x, y and z. Equation (1) is derived with combining flux and continuity equations. Also, Darcy's law is used for each fluid in soil. Therefore, advection-dispersion effects have been seen within the

governing equation. Eq. 1 for flowing single wetting phase is written as:

$$\frac{\partial p_c}{\partial x_i} = (\frac{q_{wi}\mu_w}{k_w}) + (\Delta\rho)g\frac{\partial h}{\partial x_i} \quad (2)$$

Where h is equivalent with z direction and g is the gravity acceleration for z direction. Therefore, $\frac{\partial h}{\partial x_i}$, is equal to $\frac{\partial z}{\partial x_i}$, which is $sin\,\beta$ and x_i is $\frac{h}{sin\,\beta}$ and consequently, Eq. 2 is expressed as:

$$\frac{dh_c}{dh} = 1 - \frac{|q_w|\mu_w}{(\Delta\rho)gk_w\,sin(\beta)} \quad (3)$$

Where h_c is the capillary pressure head and is equal to $\frac{p_c}{(\Delta\rho)g}$. k_w in Eq. 3 is depended on p_c and can be substituted with different equations in the literature. A schematic view of the steady downward flow of a wetting fluid (SDFWF) in unsaturated soil (Eq. 3) is presented in Fig. 1.

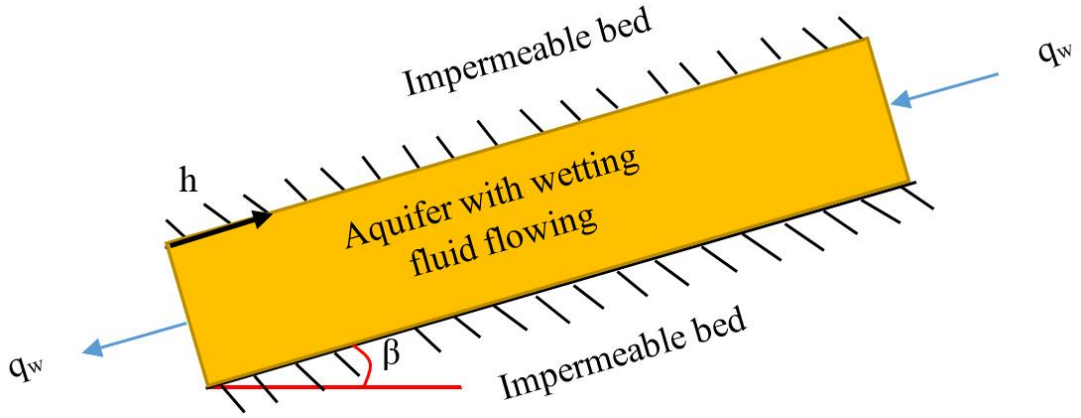


Figure 1. A schematic view of the steady downward flow of a wetting fluid (SDFWF) in unsaturated soil

In the current study, Brooks-Corey equation [33] is used for $k_w$which is:

$$k_w = k_m(\frac{P_d}{P_c})^{\eta} \quad (4)$$

Where η is $3\lambda + 2$, and λ is pore size distribution index. The typical values of λ are 2 to 5 for different soils. It should be noted that, $\lambda \to \infty$ for a soil with uniform pore size. In Eq. 4, k_m (L^2) is the saturated permeability and P_d is displacement pressure or critical P_c value. The displacement pressure is P_c value in saturation degree equal to 1. By substituting Eq. 4 to Eq. 3 and simplification, Eq. 5 is obtained:

$$\frac{dh_c}{dh} = 1 - a(\frac{h_c}{h_d})^{\eta} \quad (5)$$

Where h_d is $\frac{P_d}{(\Delta\rho)g}$ and a is:

$$a = \frac{|q_w|\mu_w}{(\Delta\rho)gk_m\,sin(\beta)} \quad (6)$$

Where a is dimensionless. To obtain the dimensionless form for Eq. 5, h_c and h should be divided by h_d. Therefore, the dimensionless form for Eq. 5 is obtained as follows:

$$\frac{dh_c^*}{dh^*} = 1 - ah_c^{*\eta} \quad (7)$$

Where h_c^* is $\frac{h_c}{h_d}$ and h^* is $\frac{h}{h_d}$. Eq. 7 is governing equation for the SDFWF in the dimensionless form. The current study presents analytical solutions for Eq. 7 in different values of η and a. The Adomian

decomposition method (ADM) is used for obtaining these analytical solutions.

3. Using the ADM for the SDFWF equation

The Adomian decomposition method presents an analytical solution to nonlinear ordinary differential equation without any simplification, linearization and change in governing equation at beginning of solution process. However, other analytical and semi-analytical methods use a simplification and linearization procedure and then present the final solution. Therefore, ADM provides very realistic and very close to reality solutions, which is one of the great advantages of this method over other analytical and semi-analytical methods. A nonlinear ordinary differential equation can be expressed in the following initial form:

$$F(y) = f \tag{8}$$

In this equation F, a nonlinear differential operator is applied to y and y itself is a function of x. Also, f itself can generally be a function of x and y. Eq. 8 can be written in more details in the form below:

$$Ly + Ry + Ny = f \tag{9}$$

In Eq. 9, L is a linear operator applied to y, for example, it can be $\frac{d}{dx}$ or $\frac{d^2}{dx^2}$. In fact, L is a linear operator as a fraction of F in Eq. 8, so that L is also invertible, i.e. if L is $\frac{d}{dx}$, it can derive the opposite action, which is integral once to x, Or, if L is $\frac{d^2}{dx^2}$, or if L is an example, it could have twice the derivative inverse of the integral of x. In Eq. 9, R is a linear operator applied to y for the remainder of the linear part F. Finally, N in Eq. 9 is a nonlinear operator; in other words, N contains nonlinear forms F. Now, by comparison of Eq. 9 with governing equation in this research (Eq. 7) and inverting the operator L, which is integral, on the sides of Eq. 9 yields:

$$L^{-1}Lh_c^* = L^{-1}f - L^{-1}Rh_c^* - L^{-1}Nh_c^* \tag{10}$$

Where L is the $\frac{d}{dh^*}$ and $L^{-1}$is the integral respect to h^*. Since the integral is associated with the integral constant and this integral constant is the initial condition of the problem, by applying the initial condition in the problem in Eq. 10, yields:

$$h_c^* = h_c^*(0) + L^{-1}f - L^{-1}Rh_c^* - L^{-1}Nh_c^* \tag{11}$$

Consequently, the final answer for h_c^* is:

$$h_c^* = \sum_{n=0}^{\infty} h_{c_n}^* = h_{c_0}^* + h_{c_1}^* + h_{c_2}^* + h_{c_3}^* + \cdots \tag{12}$$

The first two terms on the right side of Eq. 11 are introduced as $h_{c_0}^*$ in Eq. 12. This method is used for the nonlinear term Nh_c^* in Eq. 11, as follows:

$$Nh_c^* = \sum_{n=0}^{\infty} A_n\left(h_{c_0}^*, h_{c_1}^*, \ldots, h_{c_n}^*\right) = A_0 + A_1 + A_2 + \cdots \tag{13}$$

In Eq. 13, the coefficients A_0, A_1, A_2, ... are defined as:

$$A_0 = Nh_c^*(h_{c_0}^*) \tag{14a}$$

$$A_1 = h_{c_1}^* \left(\frac{d}{dh_{c_0}^*}\right) Nh_c^*(h_{c_0}^*) \tag{14b}$$

$$A_2 = h_{c_2}^* \left(\frac{d}{dh_{c_0}^*}\right) Nh_c^*(h_{c_0}^*) + \left(\frac{h_{c_1}^{*2}}{2!}\right)\left(\frac{d^2}{dh_{c_0}^{*2}}\right) Nh_c^*(h_{c_0}^*) \tag{14c}$$

$$A_3 = h_{c_3}^* \left(\frac{d}{dh_{c_0}^*}\right) Nh_c^*(h_{c_0}^*) + h_{c_1}^* h_{c_2}^* \left(\frac{d^2}{dh_{c_0}^{*2}}\right) Nh_c^*(h_{c_0}^*) + \left(\frac{h_{c_1}^{*3}}{3!}\right)\left(\frac{d^3}{dh_{c_0}^{*3}}\right) Nh_c^*(h_{c_0}^*) \tag{14d}$$

And etc. (see Adomian [34]). Now the Eq. 11 can be written as given by the Eqs. 12 and 13:

$$h_c^* = \sum_{n=0}^{\infty} h_{c_n}^* = h_{c_0}^* - L^{-1}R \sum_{n=0}^{\infty} h_{c_n}^* - L^{-1} \sum_{n=0}^{\infty} A_n \tag{15}$$

So, $h_{c_1}^*$,$h_{c_2}^*$, ... can be written as:

$$h_{c_1}^* = -L^{-1}Rh_{c_0}^* - L^{-1}A_0 \tag{16a}$$

$$h_{c_2}^* = -L^{-1}Rh_{c_1}^* - L^{-1}A_1 \tag{16b}$$

And etc. Now, by comparing Eq. 7 with the format written in Eq. 9, the parameters of Eq. 9 in this research are:

$$L = \frac{d}{dh^*}\ , R = 0\ , f = 0\ , \quad Nh_c^* = -\left(1 - ah_c^{*\eta}\right) \tag{17}$$

And the new form of Eq. 11 based on Eq. 7 is:

$$h_c^* = h_c^*(0) + L^{-1}Nh_c^* \tag{18}$$

In Eq. 18, $h_c^*(0)$ is the capillary pressure value at $h^* = 0$. Therefore, the solutions for $h_{c_1}^*$, $h_{c_2}^*$, ... are obtained in Eqs. 16a and 16b with R=0, and finally the value of h_c^* in Eq. 15 is expressed as:

$$h_c^* = h_{c_0}^* + \int A_0 dx + \int A_1 dx + \int A_2 dx + \int A_3 dx + \cdots \tag{19}$$

In Eq. 19, the second, third, fourth and etc. terms are h_{c1}^*,h_{c2}^*,h_{c3}^* and etc., respectively. Also, $h_{c_0}^*$ in Eq. 19 is the boundary condition value for Eq. 7.

4. ADM solution of SDFWF equation for λ=2 and η=8

In this section, λ is considered equal 2 and in accordance with the described process in the previous sections, η value is 8. By substituting η into Eq. 7, $f(h_{c_0}^*)$ is defined as:

$$f(h_{c_0}^*) = (1 - ah_{c_0}^{*\,8}) \tag{20}$$

According to Eq. 20 and the mentioned explanations in Eqs. 15 to 19, the answers for h_{c1}^* , h_{c2}^* , h_{c3}^* and etc. are obtained. Considering that the answers are long, only the first five terms of h_c^* in Eq. 19 are presented here:

$$h_{c_1}^* = (1 - a{h_{c_0}^*}^8)h^* \quad (21)$$

$$h_{c_2}^* = -4(1 - a{h_{c_0}^*}^8)a{h^*}^2{h_{c_0}^*}^7 \quad (22)$$

$$h_{c_3}^* = \frac{32}{3}(1 - a{h_{c_0}^*}^8){h^*}^3a^2{h_{c_0}^*}^{14} - \frac{28}{3}(1 - a{h_{c_0}^*}^8)^2{h^*}^3a{h_{c_0}^*}^6 \quad (23)$$

$$h_{c_4}^* = -8a{h_{c_0}^*}^7\left(\frac{8}{3}(1 - a{h_{c_0}^*}^8){h^*}^4a^2{h_{c_0}^*}^{14} - \frac{7}{3}(1 - a{h_{c_0}^*}^8)^2{h^*}^4a{h_{c_0}^*}^6\right) + 56(1 - a{h_{c_0}^*}^8)^2{h^*}^4a^2{h_{c_0}^*}^{13} - 14(1 - a{h_{c_0}^*}^8)^3{h^*}^4a{h_{c_0}^*}^5 \quad (24)$$

$$h_{c_5}^* = -8a{h_{c_0}^*}^7(-8a{h_{c_0}^*}^7((\frac{8}{15}(-a{h_{c_0}^*}^8 + 1))h^{*5}a^2{h_{c_0}^*}^{14} - (\frac{7}{15})(-a{h_{c_0}^*}^8 + 1)^2h^{*5}a{h_{c_0}^*}^6) + (56/5)(-a{h_{c_0}^*}^8 + 1)^2h^{*5}a^2{h_{c_0}^*}^{13} - (14/5)(-a{h_{c_0}^*}^8 + 1)^3h^{*5}a{h_{c_0}^*}^5) - 56a{h_{c_0}^*}^6((8/5)(-a{h_{c_0}^*}^8 + 1)^2h^{*5}a^2{h_{c_0}^*}^{14} + (1/5(-a{h_{c_0}^*}^8 + 1))h^{*5}((32/3(-a{h_{c_0}^*}^8 + 1))a^2{h_{c_0}^*}^{14} - (28/3)(-a{h_{c_0}^*}^8 + 1)^2a{h_{c_0}^*}^6)) + (672/5)(-a{h_{c_0}^*}^8 + 1)^3h^{*5}a^2{h_{c_0}^*}^{12} - 14(-a{h_{c_0}^*}^8 + 1)^4h^{*5}a{h_{c_0}^*}^4 \quad (25)$$

By summating these answers according to Eq. 19, the h_c^* function is obtained for λ=2 and η=8. In order to plot h_c^* verses h^*, example values for a and h_{c0}^* should be selected. These values are selected based on discharge value and soil properties. By considering a=0.1, 0.5 and 0.7 and h_{c0}^* (boundary condition) equal to 1 in these answers, h_c^*functions for the approximately eighth sentences are presented in Table 1.

Table 1. h_c^* functions for different values of *a* in *λ=2* and *η=8*

Values for *a*	Values for h_{c0}^*	h_c^* functions
0.1	1	$h_c^* = 1 + 0{,}9h^* - 0{,}36{h^*}^2 - 0{,}66{h^*}^3 - 0{,}435{h^*}^4 + 0{,}72354{h^*}^5 + 1{,}891052{h^*}^6 + 0{,}8468553721{h^*}^7$
0.5	1	$h_c^* = 1 + 0{,}5h^* - 1{,}00{h^*}^2 + 0{,}166666666{h^*}^3 + 2{,}458333334{h^*}^4 - 1{,}470833331{h^*}^5 - 8{,}790277781{h^*}^6 + 9{,}669543642{h^*}^7$
0.7	1	$h_c^* = 1 + 0{,}3h^* - 0{,}84{h^*}^2 + 0{,}98{h^*}^3 + 0{,}833{h^*}^4 - 4{,}30514{h^*}^5 + 2{,}611046666{h^*}^6 + 13{,}51103507{h^*}^7$

Replacing h^* values in the analytical solutions (Table 1), the dimensionless capillary pressure head (h_c^*) can be plotted. Figure 2 shows a comparison of h_c^*values using ADM (Table 1) and numerical solution values (to Eq. 7) for a dimensionless length (h^*) of 0.5 in a vertical soil column with $\beta = 90°$. Finite difference method (FDM) with $\Delta h^* = 0.01$is used for the numerical solution. As shown in Figure 2, there is an excellent agreement between ADM and FDM results. The comparison confirms high accuracy of h_c^* functions in Table 1 as analytical solutions for SDFWF equation with soil properties of λ=2 and η=8.

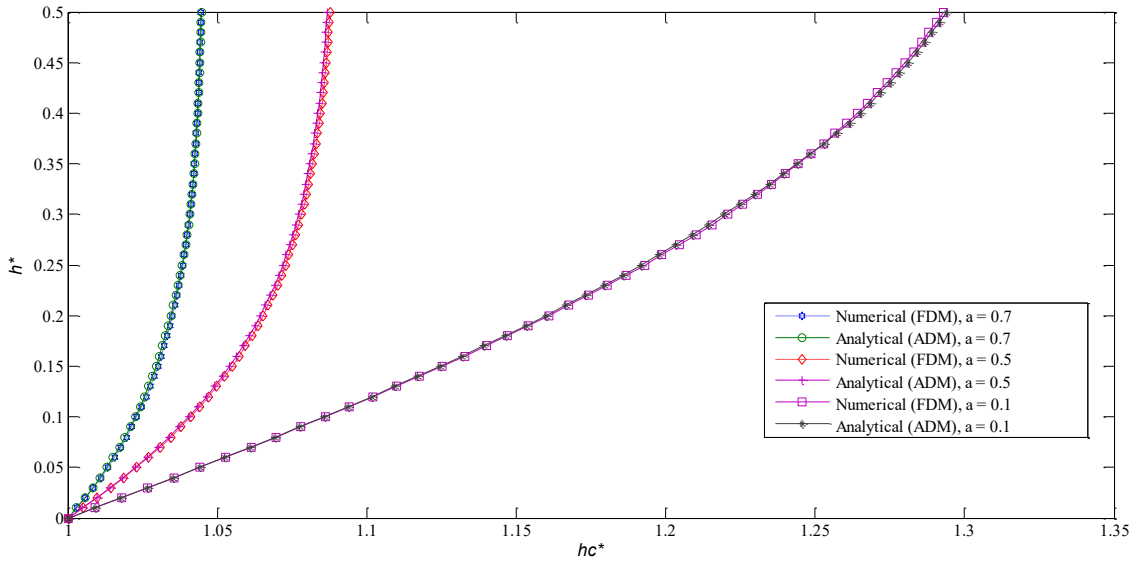


Figure 2. Comparison of normalized capillary pressures head verses normalized elevation values in numerical and analytical methods for λ=2 and η=8

5. ADM solution of SDFWF equation for λ=3 and η=11

In this section, λ is considered equal 3 and in accordance with the described process in the previous sections, η value is 11. By substituting η into Eq. 7, $f(h_{c_0}^*)$ is defined as:

$$f(h_{c_0}^*) = (1 - a{h_{c_0}^*}^{11}) \quad (26)$$

According to Eq. 26 and the mentioned explanations in Eqs. 15 to 19, the answers for h_{c1}^*, h_{c2}^*, h_{c3}^* and etc. are obtained. Considering that the answers are long, only the first four terms of h_c^* in Eq. 19 are presented here:

$$h_{c_1}^* = (1 - a{h_{c_0}^*}^{11})h^* \quad (27)$$

$$h_{c_2}^* = -\frac{11}{2}\left(1 - a{h_{c_0}^*}^{11}\right){h^*}^2 a{h_{c_0}^*}^{10} \quad (28)$$

$$h_{c_3}^* = \frac{121}{6}\left(1 - a{h_{c_0}^*}^{11}\right){h^*}^3 a^2{h_{c_0}^*}^{20} - \frac{55}{3}\left(1 - a{h_{c_0}^*}^{11}\right)^2 {h^*}^3 a{h_{c_0}^*}^{9} \quad (29)$$

$$h_{c_4}^* = -11a{h_{c_0}^*}^{10}\left(\frac{121}{24}\left(1 - a{h_{c_0}^*}^{11}\right){h^*}^4 a^2{h_{c_0}^*}^{20} - \frac{55}{12}\left(1 - a{h_{c_0}^*}^{11}\right)^2 {h^*}^4 a{h_{c_0}^*}^{9}\right) + \frac{605}{4}\left(1 - a{h_{c_0}^*}^{11}\right)^2 {h^*}^4 a^2{h_{c_0}^*}^{19} - \frac{165}{4}\left(1 - a{h_{c_0}^*}^{11}\right)^3 {h^*}^4 a{h_{c_0}^*}^{8} \quad (30)$$

By summating these answers according to Eq. 19, the h_c^* function is obtained for λ=3 and η=11. In order to plot h_c^* verses h^*, example values for a and $h_{c_0}^*$ should be selected. These values are selected based on discharge value and soil properties. By considering a=0.1, 0.5 and 0.7 and $h_{c_0}^*$ (boundary condition) equal to 1 in these answers, h_c^* functions for the approximately eighth sentences are presented in Table 2.

Table 2- h_c^* functions for different values of a in $\lambda=3$ and $\eta=11$

Values for a	Values for $h_{c_0}^*$	h_c^* functions
0.1	1	$h_c^* = 1 + 0.9h^* - 0.495{h^*}^2 - 1.3035{h^*}^3 - 1.4235375{h^*}^4 + 2.26372575{h^*}^5 + 11.03425936{h^*}^6 + 12.36402593{h^*}^7$
0.5	1	$h_c^* = 1 + 0.5h^* - 1.375000000{h^*}^2 + 0.229166666{h^*}^3 + 6.559895834{h^*}^4 - 3.921614573{h^*}^5 - 47.23721789{h^*}^6 + 51.09599910{h^*}^7$
0.7	1	$h_c^* = 1 + 0.3h^* - 1.155{h^*}^2 + 1.8095{h^*}^3 + 2.4072125{h^*}^4 - 15.50947475{h^*}^5 + 9.61202517{h^*}^6 + 101.8603676{h^*}^7$

Substituting h^* values in the analytical solutions (Table 2), the dimensionless capillary pressure head (h_c^*) may be plotted. Figure 3 shows a comparison of h_c^* values using ADM (Table 2) and numerical solution values (to Eq. 7) for a dimensionless length (h^*) of 0.5 in a vertical soil column with $\beta = 90°$. Finite difference method (FDM) with $\Delta h^* = 0.01$is used for the numerical solution. As shown in Figure 3, there is an excellent agreement between ADM and FDM results. The comparison confirms accuracy of h_c^* functions in Table 2 as analytical solutions for SFWF equation with soil properties of λ=3 and η=11.

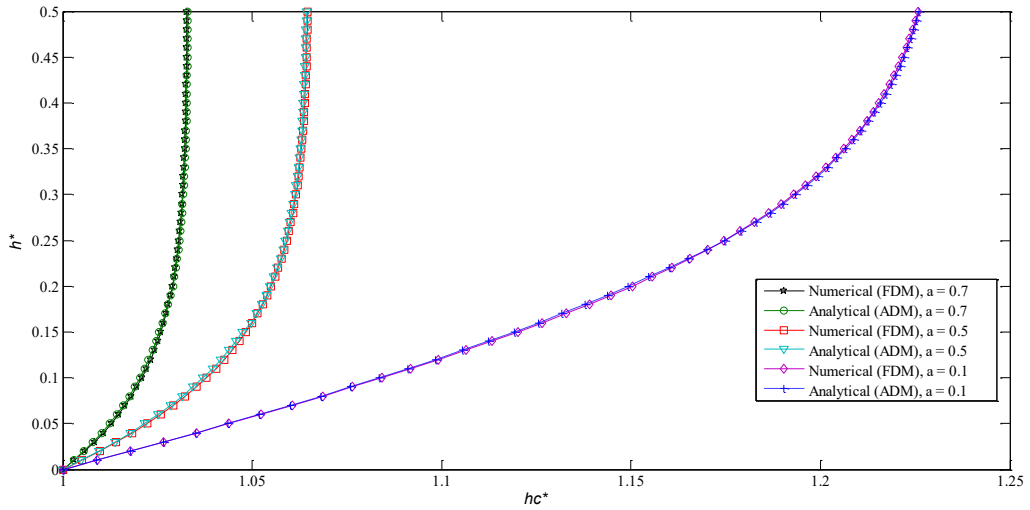


Figure 3. Comparison of normalized capillary pressures head verses normalized elevation values in numerical and analytical methods for λ=3 and η=11

6. ADM solution of SDFWF equation for λ=4 and η=14

In this section, λ is considered equal 4 and in accordance with the described process in the previous sections, η value is 14. By substituting η into Eq. 7, $f(h_{c_0}^*)$ is defined as:

$$f(h_{c_0}^*) = (1 - a{h_{c_0}^*}^{14}) \quad (31)$$

According to Eq. 31 and the mentioned explanations in Eqs. 15 to 19, the answers for h_{c1}^* , h_{c2}^* , h_{c3}^* and etc. are obtained. Considering that the answers are long, only the first four terms of h_c^* in Eq. 19 are presented here:

$$h_{c_1}^* = (1 - a{h_{c_0}^*}^{14})h^* \quad (32)$$

$$h_{c_2}^* = -7\left(1 - a{h_{c_0}^*}^{14}\right){h^*}^2 a{h_{c_0}^*}^{13} \quad (33)$$

$$h_{c_3}^* = \frac{98}{3}\left(1 - a{h_{c_0}^*}^{14}\right){h^*}^3 a^2{h_{c_0}^*}^{26} - \frac{91}{3}\left(1 - a{h_{c_0}^*}^{14}\right)^2 {h^*}^3 a{h_{c_0}^*}^{12} \quad (34)$$

$$h_{c_4}^* = -14a{h_{c_0}^*}^{13}\left(\frac{49}{6}\left(1 - a{h_{c_0}^*}^{14}\right){h^*}^4 a^2{h_{c_0}^*}^{26} - \frac{91}{12}\left(1 - a{h_{c_0}^*}^{14}\right)^2 {h^*}^4 a{h_{c_0}^*}^{12}\right) + \frac{637}{2}\left(1 - a{h_{c_0}^*}^{14}\right)^2 {h^*}^4 a^2{h_{c_0}^*}^{25} - 91\left(1 - a{h_{c_0}^*}^{14}\right)^3 {h^*}^4 a{h_{c_0}^*}^{11} \quad (35)$$

By summating these answers according to Eq. 19, the h_c^* function is obtained for λ=4 and η=14. In order to plot h_c^* verses h^*, example values for a and $h_{c_0}^*$ should be selected. These values are selected based on discharge value and soil properties. By considering a=0.01, 0.001 and 0.0001 and $h_{c_0}^*$ (boundary condition) equal to 1 in these answers, h_c^* functions for the approximately eighth sentences are presented in Table 3.

Table 3. h_c^* functions for different values of *a* in *λ=4* and *η=14*

Values for a	Values for $h_{c_0}^*$	h_c^* functions
0.01	1	$h_c^* = 1 + 0.99h^* - 0.0693{h^*}^2 - 0.294063{h^*}^3 - 0.8414637{h^*}^4 - 1.646118428{h^*}^5 - 1.923599743{h^*}^6 + 0.1642565113{h^*}^7$
0.001	1	$h_c^* = 1 + 0.999h^* - 0.006993{h^*}^2 - 0.030240063{h^*}^3 - 0.09030356937{h^*}^4 - 0.1965245847{h^*}^5 - 0.3186765805{h^*}^6 - 0.3795618968{h^*}^7$
0.0001	1	$h_c^* = 1 + 0.9999h^* - 0.00069993{h^*}^2 - 0.003032400063{h^*}^3 - 0.00909302457{h^*}^4 - 0.0199831278{h^*}^5 - 0.03321588658{h^*}^6 - 0.04240053504{h^*}^7$

Substituting h^* values in the analytical solutions (Table 3), the dimensionless capillary pressure head (h_c^*) may be plotted. Figure 4 shows a comparison of h_c^* values using ADM (Table 3) and numerical solution values (to Eq. 7) for a dimensionless length (h^*) of 1.5 in a vertical soil column with $\beta = 90°$. Finite difference method (FDM) with $\Delta h^* = 0.01$is used for the numerical solution. As shown in Figure 4, there is an excellent agreement between ADM and FDM results. The comparison confirms high accuracy of h_c^* functions in Table 3 as analytical solutions for SFWF equation with soil properties of λ=4 and η=14. By comparing Figures 2, 3, and 4, it is found that as the values of λ and η increase, the graph slope of h^* versus h_c^* increase. Also, by increasing λ, the graphs at high values for h^* are formed as almost straight vertical lines. In other words, as the pore size distribution index (λ) increases, the pore size of the soil increases and the flow rate passes through the soil column at a faster rate.

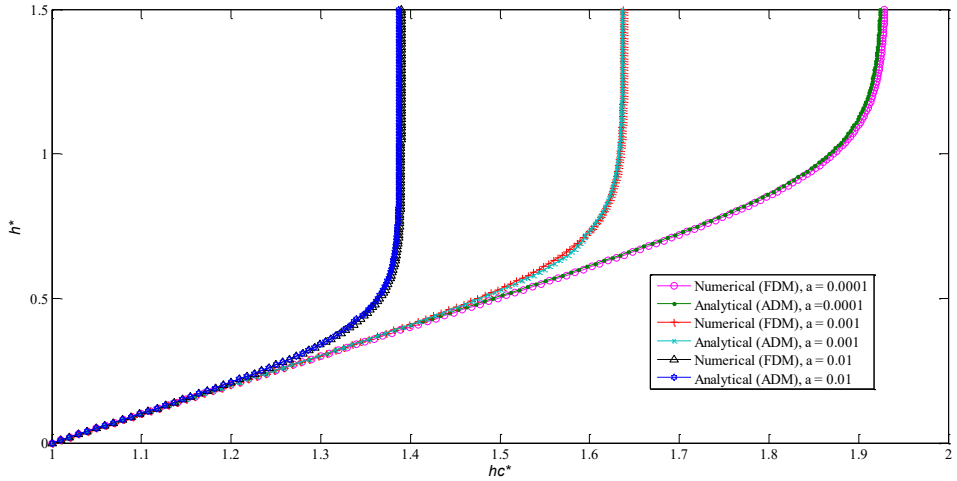


Figure 4. Comparison of normalized capillary pressures head verses normalized elevation values in numerical and analytical methods for λ=4 and η=14

Conclusion

This paper presented analytical solutions for the steady downward flow of a wetting fluid (SDFWF) in unsaturated soil. Governing equation for SFWF is an ordinary differential equation with strongly nonlinear form and therefore, presenting analytical solutions for this equation is very important. The Adomian decomposition method (ADM) were applied to SDFWF equation for obtaining analytical solutions. A total of 3 cases were considered in this study for different soil properties. The pore size distribution index in these cases were 2, 3 and 4. A comparison between ADM and finite difference method (FDM) results were performed in three cases. An excellent agreement between ADM and FDM results were seen in all cases. Therefore, it was concluded that ADM may be used to obtain analytical solutions for SFWF equation in vertical soil column with a high level of accuracy. Presented analytical solutions in this research can be used as reference solutions for efficiency assessment of various numerical techniques and similar laboratory works that calculate capillary pressure distribution in soil column with SFWF.

Funding statement:

This research received no external funding.

Conflict of Interest:

The authors declare that they have no conflict of interest.

AI Statement:

During the preparation of this work the author used check spelling tools in order to grammar correct. After using this tool, the author reviewed and edited the content as needed and takes full responsibility for the content of the publication.

Author Contributions:

All authors contributed to the study conception and design. Material preparation, data collection, and analysis … were performed by Hamed Reza Zarif Sanayei. The first draft of the manuscript was written by Hamed Reza Zarif Sanayei. The author reads and approved the final manuscript.

References

1. Van Duijn CJ, Pieters GJM, Raats PAC. Steady flows in unsaturated soils are stable. Transport in Porous Media. 2004; 57:215–244. https://doi.org/10.1023/B:TIPM.0000038250.72364.20
2. Szymkiewicz A, Helmig R, Kuhnke H. Two-phase flow in heterogeneous porous media with non-wetting phase trapping. Transport in Porous Media. 2011;86: 27–47. https://doi.org/10.1007/s11242-010-9604-x
3. Du X, Nydal OJ. Flow models and numerical schemes for single/two-phase transient flow

in one dimension. Applied Mathematical Modelling. 2017; 42:145–160. https://doi.org/10.1016/j.apm.2016.10.017
4. Cogswell DA, Szulczewski ML. Simulation of incompressible two-phase flow in porous media with large time steps. Journal of Computational Physics. 2017; 345:856–865. https://doi.org/10.1016/j.jcp.2017.06.007
5. Zhang H, Lan H, Lin N. A numerical simulation of water distribution associated with internal corrosion induced by water wetting in upward inclined oil pipes. Journal of Petroleum Science and Engineering. 2019; 173:351–361. https://doi.org/10.17632/6h5nzf9zb4.1
6. Ma T, Jiang L, Shen W, Cao WZ, Guo C, Nick HM. Fully coupled hydro-mechanical modeling of two-phase flow in deformable fractured porous media with discontinuous and continuous Galerkin method. Computers and Geotechnics. 2023; 164:105823. https://doi.org/10.1016/j.compgeo.2023.105823
7. Ghedira A, Lataoui Z, Benselama AM, Bertin Y, Jemni A. Numerical simulation of incompressible two-phase flows with phase change process in porous media. Results in Engineering. 2025; 25: 103706. https://doi.org/10.1016/j.rineng.2024.103706
8. Rao X, Cheng L, Cao R, Song W, Du X, He Y, Dai D. Numerical simulation of two-phase flow in porous media based on mimetic Green element method. Engineering Analysis with Boundary Elements. 2019; 101: 113-120. https://doi.org/10.1016/j.enganabound.2019.01.010
9. Tran LK, Kim JC, Matthäi SK. Simulation of two-phase flow in porous media with sharp material discontinuities. Advances in Water Resources. 2020; 142: 103636. https://doi.org/10.1016/j.advwatres.2020.103636
10. Lee EJ, Wang W, Chen P, Jiao Z, Gong Y, Mu D, Liao WY. Mesh-free simulation of two-phase fluid flow in porous media based on the shock-fitting method. Journal of Petroleum Science and Engineering. 2022; 215(B): 110637. https://doi.org/10.1016/j.petrol.2022.110637
11. Li X, Li L, Ma W, Wang W. Two-phase flow patterns identification in porous media using feature extraction and SVM. International Journal of Multiphase Flow. 2022; 156: 104222. https://doi.org/10.1016/j.ijmultiphaseflow.2022.104222
12. Shen B., Riviere B. A sequential discontinuous Galerkin method for two-phase flow in deformable porous media. Computer Methods in Applied Mechanics and Engineering. 2022; 399: 115266. https://doi.org/10.1016/j.cma.2022.115266
13. Ballini E, Formaggia L, Fumagalli A, Keilegavlen E, Scotti A. A hybrid upwind scheme for two-phase flow in fractured porous media. Computer Methods in Applied Mechanics and Engineering. 2024; 432: 117437. https://doi.org/10.1016/j.cma.2024.117437
14. Feng J., Liu Y., Min J. A pore-scale investigation of viscous coupling effect on immiscible two-phase flow in porous media. Chemical Engineering Research and Design. 2024; 211: 379-390. https://doi.org/10.1016/j.cherd.2024.10.019
15. Zhan W, Zhao H, Liu Y, Wei Z, Rao X. A novel meshless numerical simulation of oil-water two-phase flow with gravity and capillary forces in three-dimensional porous media. Engineering Analysis with Boundary Elements. 2024; 169(A): 105975. https://doi.org/10.1016/j.enganabound.2024.105975
16. Li X, Yan Y, Chen H. A class of high-order physics-preserving schemes for thermodynamically consistent model of incompressible and immiscible two-phase flow in porous media. Journal of Computational Physics. 2025; 529: 113864. https://doi.org/10.1016/j.jcp.2025.113864
17. Peng J, Xia B, Lu Y, Song R, Wang L. Pore-scale analysis and modeling of heterogeneous wettability in immiscible two-phase flow inside natural porous media. Geoenergy Science and Engineering. 2025; 247: 213676. https://doi.org/10.1016/j.geoen.2025.213676
18. Vakili A. H., Falamaki A. An investigation on the parameters affecting the behavior of broadly graded, dispersive base soil-filter systems in earth dams. Journal of Hydraulic structures. 2025; 11(32): 44-60. https://doi.org/10.22055/JHS.2024.46910.1299
19. Mohtashami A., Hashemi Monfared S. A., Azizyan G., Akbarpour A. Estimation of Parameters in Groundwater Modeling by Particle Filter linked to the meshless local

Petrov-Galerkin Numerical Method. Journal of Hydraulic structures. 2021; 7(15): 16-37. https://doi.org/10.22055/JHS.2021.37091.1167

20. Talebi M. Investigating the vulnerability of underground water to pollution (case study: East and Northeast of Chaharmahal and Bakhtiari province). Journal of Hydraulic structures. 2025; 11(32): 87-105. https://doi.org/10.22055/JHS.2024.47643.1316
21. Pan L, Webb SW, Oldenburg CM. Analytical solution for two-phase flow in a wellbore using the drift-flux model. Advances in Water Resources. 2011; 34(12): 1656-1665. https://doi.org/10.1016/j.advwatres.2011.08.009
22. Borazjani S, Bedrikovetsky P, Farajzadeh R. Analytical solutions of oil displacement by a polymer slug with varying salinity. Journal of Petroleum Science and Engineering. 2016; 140: 28–40. https://doi.org/10.1016/j.petrol.2016.01.001
23. Fučík R, llangasekare TH, Beneš M. Multidimensional self-similar analytical solutions of two-phase flow in porous media. Advances in Water Resources. 2016; 90: 51-56. https://doi.org/10.1016/j.advwatres.2016.02.007
24. Mohammadein SA, Shalaby GA, Abu-Bakr AF, Abu-Nab AK. Analytical solution of gas bubble dynamics between two-phase flow. Results in Physics. 2017; 7: 2396-2403. https://doi.org/10.1016/j.rinp.2017.07.007
25. Hajra SG, Kandel S, Pudasaini SP. On analytical solutions of a two-phase mass flow model. Nonlinear Analysis: Real World Application. 2018; 41: 412-427. https://doi.org/10.1016/j.nonrwa.2017.09.009
26. Rybdylova O, Sazhin SS, Osiptsov AN, Kaplanski FB, Begg S, Heikal M. Modelling of a two-phase vortex-ring flow using an analytical solution for the carrier phase. Applied Mathematics and Computation. 2018; 326: 159-169. https://doi.org/10.1016/j.amc.2017.12.044
27. Rabinovich A. An analytical solution for cyclic flow of two immiscible phases. Journal of Hydrology. 2019; 570: 682-691. https://doi.org/10.1016/j.jhydrol.2018.12.056
28. Zarif Sanayei HR, Talebbeydokhti N, Rakhshandehroo GR. Analytical solutions for water infiltration into unsaturated–semi-saturated soils under different water content distributions on the top boundary. Iranian Journal of Science and Technology, Transactions of Civil Engineering. 2019; 43: 747-760. https://doi.org/10.1007/s40996-019-00245-3
29. Apolinário FD, Paula AS, Pires AP. Injection of water slug containing two polymers in porous media: Analytical solution for two-phase flow accounting for adsorption effects. Journal of Petroleum Science and Engineering. 2020; 188: 106927. https://doi.org/10.1016/j.petrol.2020.106927
30. Barros WQ, Pires AP, Peres AMM. Analytical solution for one-dimensional three-phase incompressible flow in porous media for concave relative permeability curves. International Journal of Non-Linear Mechanics. 2021; 137: 103792. https://doi.org/10.1016/j.ijnonlinmec.2021.103792
31. Yang Y, Xu Y, Yuan C, Wang J, Wu H, Zhang T. Water cut measurement of oil–water two-phase flow in the resonant cavity sensor based on analytical field solution method. Measurement. 2021; 174: 109078. https://doi.org/10.1016/j.measurement.2021.109078
32. Zarif Sanayei HR, Javdanian H, Rakhshandehroo GR. Assessment of confined aquifer response to recharge variations and water inflow distributions using analytical approach. Environmental Science and Pollution Research. 2021; 28:50878–50889. https://doi.org/10.1007/s11356-021-14314-6
33. Corey AT. Mechanics of immiscible fluids in porous media. Water Resources Publications, LLC, Colorado, USA; 1994.
34. Adomian G. Nonlinear Stochastic Operator Equations. Academic Press, USA; 2014

© 2025 by the authors. Licensee SCU, Ahvaz, Iran. This article is an open access article distributed under the terms and conditions of the Creative Commons Attribution 4.0 International (CC BY 4.0 license) (http://creativecommons.org/licenses/by/4.0/).